

ISTITUTO NAZIONALE DI FISICA NUCLEARE

Sezione di Lecce

INFN/BE-97/01
13 Febbraio 1997

R. Perrino:
**ELECTRON INDUCED HEXADECAPOLE EXCITATIONS IN NEODYMIUM
ISOTOPES**

PACS: 21.10.-k, 21.10.Re, 21.60.Ev, 25.30.Dh, 27.60.+j, 27.70.+q

*SIS-Pubblicazioni
dei Laboratori Nazionali di Frascati*

INFN – Istituto Nazionale di Fisica Nucleare
Sezione di Lecce

INFN/BE-97/01
13 Febbraio 1997

**ELECTRON INDUCED HEXADECAPOLE EXCITATIONS IN
NEODYMIUM ISOTOPES**

R. Perrino

INFN–Sezione di Lecce, I-73100 Lecce (Italy)

ABSTRACT

The low-lying hexadecapole states in the stable even-even Neodymium isotopes have been investigated by means of inelastic electron scattering. The radial shapes of the extracted transition charge densities display a systematic behaviour, with clear differences among the various hexadecapole states of the same isotope, and analogies among hexadecapole states of different isotopes. The analysis of the experimental results within the interacting *sdg*-boson model gives information on the structure functions of the different boson-pair configurations involved in the hexadecapole excitations.

The structure of nuclear excited states can be investigated by studying the radial shape of the transition charge density, measured from high resolution inelastic electron scattering. The excitation of the low-lying hexadecapole states can be described introducing four structure functions in the framework of the classical sd -interacting boson model (IBA) expanded with only one g -boson. The function $\alpha_{dd}(r)$ is related to a recoupling of two d -bosons, and, in vibrational nuclei, is the main component of the 4_1^+ level, which belongs to the well-known two-quadrupole-phonon triplet. Collective models predict for two-phonon configurations a shape of the second derivative (∂'') of the ground state (gs) charge density. The functions $\alpha_{sg}(r)$ and $\alpha_{dg}(r)$, related to the exchange of one s - or d -boson with one g -boson, are expected to have a shape similar to the first derivative (∂') of the gs density, the shape predicted by collective models for one-phonon configurations. These configurations constitute the main components of higher 4^+ states, but can also influence the 4_1^+ wave function if a mixing among the different configurations is introduced in the hamiltonian of the model. The second-order $\alpha_{gg}(r)$ function is also introduced by the IBA model when the hexadecapole degree of freedom, namely the g -boson, is added to the sd -expansion.

This work is intended to investigate the radial shape of the sdg -IBA hexadecapole structure functions in transitional nuclei. The even-even Nd isotopes constitute a good test-case for such an investigation, since two transitions are involved in the chain: a spherical-collective ($A=142$ to $A=146$) and a vibrational-rotational ($A=146$ to $A=150$), respectively.

The transition charge densities in the $^{142,144,146,148,150}\text{Nd}$ have been derived from high-energy inelastic electron scattering experiments, performed at the NIKHEF-K using the QDD magnetic spectrometer. Results from these experiments on $^{142,144,146,150}\text{Nd}$ have been published elsewhere [4-7]. The effective transferred momentum in the experiments ranged between 0.5 and 2.8 fm^{-1} . Targets of approximately 10 mg/cm^2 were used. An energy resolution of about 12 keV was achieved for the lowest incident electron energy (112 MeV), and up to about 30 keV for the highest energy (450 MeV). The identification of the excited states observed was checked against the results of a recent investigation [8] on these nuclei performed with inelastic scattering of protons and deuterons. A comparison with the results from ref. 8 suggests that, in the present electron scattering experiment, the strongest levels in each nucleus have been observed. The transition charge densities were deduced through a Fourier-Bessel analysis of the cross sections, as detailed in ref. 4. The analysis accounted for the incompleteness of the q -range using a high- q constraint.

The extracted hexadecapole transition charge densities $\rho_4(r)$ for the strongest transitions are shown in Fig. 1. The densities display in general roughly a ∂' shape with no clear evidence

for a ∂'' shape. However, the densities peak at different radial extensions, and some of them display a more complex structure involving a small inner peak.

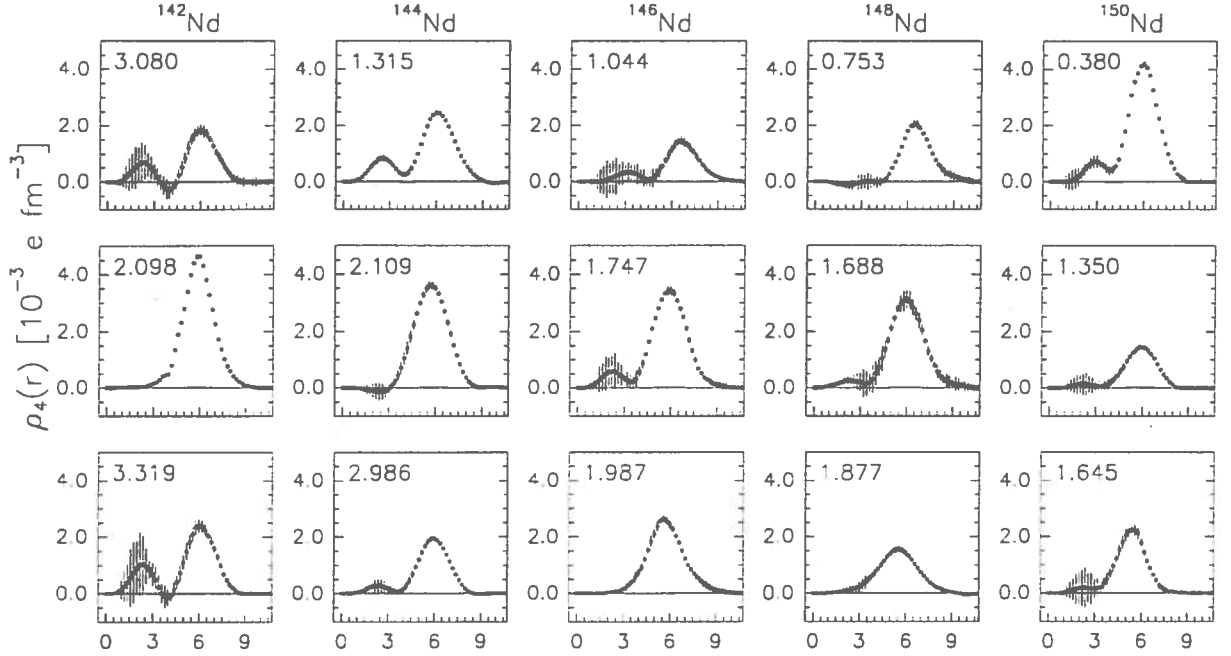


Fig. 1 Transition charge densities of some low-lying hexadecapole excitations in the five investigated Nd isotopes. The densities are labelled by the excitation energy (in MeV) of the relative level. The densities belonging to the same isotope are given in one column, ordered by excitation energy, with the exception of ^{142}Nd .

Aiming at a comparison of the hexadecapole measured densities with a collective model prediction, it is mandatory to consider the experimental $B(E4)$ distributions as a function of excitation energy, as shown in Fig. 2. The $B(E\lambda)$ are evaluated from the transition charge density through the equation:

$$B(E\lambda) = \frac{2J_f + 1}{2J_i + 1} \left[\int \rho_\lambda(r) r^{\lambda+2} dr \right]^2 \quad (1)$$

The theoretical expectations have been calculated within the frame of the IBA, using the following hamiltonian to couple the g -boson the sd -core:

$$H_{sdg} = H_{sd} + \epsilon_g (g+\tilde{g})^{(0)} + \gamma [(g+\tilde{g})^{(2)} (d+\tilde{d})^{(2)}]^{(0)} + \zeta [(g+s)^{(4)} (\tilde{d}\tilde{d})^{(4)} + (d+d^+)^{(4)} (\tilde{g}\tilde{s})^{(4)}]^{(0)} \quad (2)$$

where the *sd*-hamiltonian is expressed as a multipole expansion, ϵ_g is the *g*-boson energy and the last two terms of the *sdg* interaction are the leading ones of a more complete *g*-boson hamiltonian that is used in the consistent Q-formalism [10].

The electromagnetic transition operators are given by the extension of the usual *sd*-operators [9]:

$$T(E2) = (s+\tilde{d} + d+\tilde{s})^{(2)} + Q2DD(d+\tilde{d})^{(2)} + Q2DG(g+\tilde{d} + d+\tilde{g})^{(2)} + Q2GG(g+\tilde{g})^{(2)} \quad (3)$$

$$T(E4) = (d+\tilde{d})^{(4)} + Q4SG(g+\tilde{s} + s+\tilde{g})^{(4)} + Q4DG(g+\tilde{d} + d+\tilde{g})^{(4)} + Q4GG(g+\tilde{g})^{(4)} \quad (4)$$

In addition to the *sd*-approximation, eqs. 3 and 4 include the new *sg*, *dg*, and *gg* modes introduced by the *g*-boson to form $L=2$ and 4 angular momenta. The reduced transition probabilities are evaluated from the transition operators through the usual polarisation charges: $B(E2) = (e_2 \langle 2^+ || T(E2) || 0_{gs}^+ \rangle)^2$; $B(E4) = (e_4 \langle 4^+ || T(E4) || 0_{gs}^+ \rangle)^2$.

In the previous equations the additional parameters introduced with the *g*-boson, act in the following way: ϵ_g shifts the excitation energies of the 4^+ states belonging to the *sg*, *dg*, and *gg* *g*-boson configurations (Γ states) with respect to the *dd* *sd*-boson ones (Σ states); the parameter ζ influences only slightly the position of the levels, but causes both the mixing between the pure *sd*- and *g*-configurations and, at high values, the splitting of the pure or degenerate *g*-configurations; the parameter γ influences strongly the relative energy of the different *g*-boson configurations. The *Q2DG*, *Q2GG*, *Q4SG*, *Q4DG*, and *Q4GG* polarisation charges normalise the strengths of the corresponding boson-pair configurations, and do not influence the excited level sequence.

The relevant part of the distributions in Fig. 2 is reproduced by the set of *sd*- IBA-1 parameters and by the values of ϵ_g , γ , ζ given in Table I. According to this interpretation, most of the hexadecapole strength is concentrated into a few levels, each with a predominant boson pair configuration, owing to the small mixing of the *sd*- and *g*- configurations. In particular, all the 4_1^+ states are *dd*, with the exception of ^{142}Nd , where, in the 4_1^+ , the *sg* strength is allocated.

It is worth noting that also the quasiparticle-phonon model (QPM) [13] describes [4] the first 4^+ state in ^{142}Nd as a one-phonon hexadecapole state at 2.160 MeV and allocates the two-quadrupole-phonon hexadecapole strength into two levels at 3.160 and 3.460 MeV. Furthermore, the transition charge density of the level 4_2^+ at $E_x=3.080$ MeV in ^{142}Nd is similar to that of the 4_1^+ states of the other Nd isotopes (first row of Fig. 1), while the shape of the

transition density of the 4_1^+ state in ^{142}Nd at $E_x=2.098$ MeV is similar to that of the higher 4^+ states of the other Nd isotopes, displayed in the second row of Fig. 1.

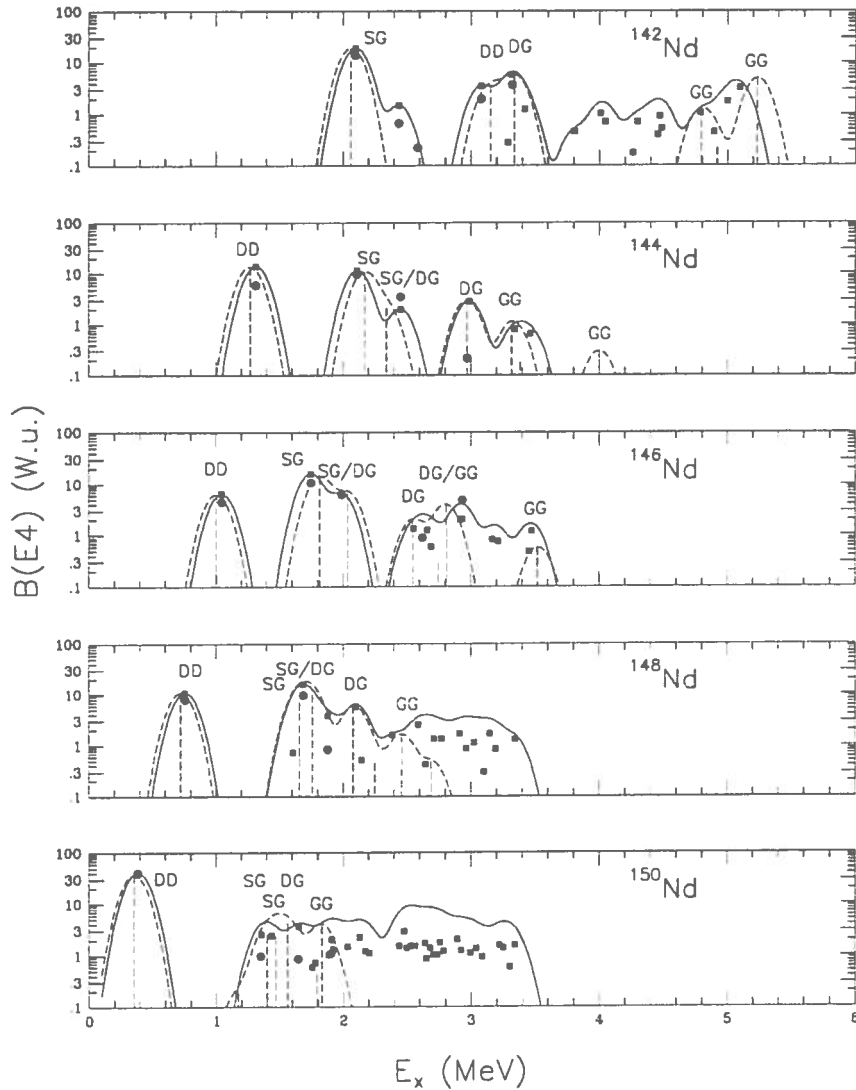


Fig. 2 $B(E4)$ values as a function of excitation energy. Full points are data from Ref. 8, full squares are from the present work. The data have been smeared using gaussians 200 keV wide (full line) to show level clustering in basic boson configurations (sg, dd, dg, gg). Results from IBA analysis are shown as dashed vertical lines and a smeared dashed curve.

With the exception of the value of γ for ^{142}Nd , all the other g -boson parameters in Table I have smooth $N_V \cdot N_\pi$ dependences. The choice of the parameters for the transition operator $T(E4)$ (eq. 4) is an open problem. As discussed in ref. 14, simple microscopic evaluations give values near to 1 for the parameters $Q4SG$, $Q4DG$ and $Q4GG$. In the present analysis values of this order have been found for $Q4DG$, but the experiment clearly requires smaller $Q4SG$ values. Moreover some improvement at high excitation energies is obtained using very large $Q4GG$ values. This parameter can be reduced by increasing the hexadecapole term HEX in the

sd-hamiltonian. However its value remains very high. A large, and probably unphysical, Q4GG value could be due to a too limited model space, it is to say to the need of more *g*-bosons. In this case the contribution of the *gg* configuration is overestimated and therefore it is not reliably evaluated in the present analysis. This possibility limits the hexadecapole strength which can be fitted with only one *g*-boson to an excitation energy of 3.6 MeV for ^{142}Nd , down to 1.7 MeV for ^{150}Nd . It is worth noting that the QPM calculations [4] predict that the hexadecapole strength distributions for ^{142}Nd are due to seven hexadecapole one-phonon configurations.

TABLE I IBA parameters used in the codes [9] PHINTL and FBEML for the *sdg*-analyses described in the text.

parameter	isotope	142	144	146	148	150
H_d (keV)		1626	816	743	605	369
PAIR (keV)		0.0	0.0	0.0	0.0	0.0
ELL (keV)		0.0	0.0	1.9	1	-0.4
QQ (keV)		-74	-92	-71.4	-53.6	-38.9
OCT (keV)		-3.5	-2.2	-0.5	0.7	1.1
HEX (keV)		2	2.2	2.7	3.7	4.5
CHQ		-1.0	-1.1	-1.34	-2.24	-2.46
ε_g (MeV)		2.08	1.95	1.65	1.53	1.20
γ (MeV)		2.0	0.0	0.0	0.0	0.0
ζ (MeV)		0.25	0.3	0.3	0.1	0.01
e_4 (eb ²)		0.07	0.18	0.13	0.09	0.12
Q4SG		0.53	0.09	0.17	0.30	0.10
Q4DG		6.45	0.66	0.94	1.02	0.50
Q4GG		4212.	26.7	30.1	43.4	210.

The matrix elements evaluated from the *sdg*-analysis and the experimental charge transition densities in Fig. 1 have been used to evaluate the radial shapes of the structure functions $\alpha_{dd}(r)$, $\alpha_{sg}(r)$ and $\alpha_{dg}(r)$. This is done by equating at several radii:

$$\langle 4^+ || \rho_4^{\text{IBA}}(r) || 0_{gs}^+ \rangle = \rho_4^{\text{exp}}(r) \quad (5)$$

for each of the three experimental densities for every nucleus (given in the various columns of Fig. 1), and with the r-dependent operator defined as:

$$\rho_4^{\text{IBA}}(r) = e_4 [(d+\tilde{d})^{(4)} \alpha_{\text{DD}}(r) + Q4\text{SG}(g+\tilde{s} + s+\tilde{g})^{(4)} \alpha_{\text{SG}}(r) + Q4\text{DG}(g+\tilde{d} + d+\tilde{g})^{(4)} \alpha_{\text{DG}}(r)] \quad (6)$$

The solutions resulting from this procedure are dependent upon the algebraic sign which is attributed to the different experimental densities. This, unfortunately, cannot be obtained from electron scattering cross sections. The first five columns in Fig. 3 give a possible solution for $\alpha_{\text{dd}}(r)$, $\alpha_{\text{sg}}(r)$ and $\alpha_{\text{dg}}(r)$.

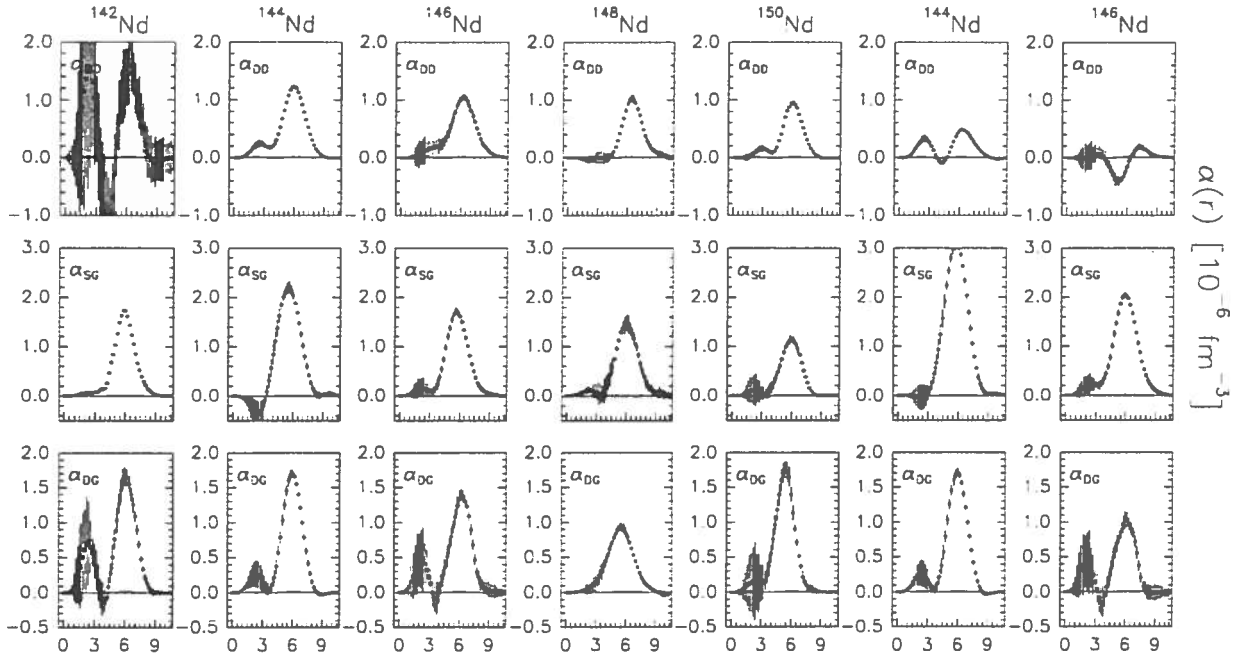


Fig. 3 Hexadecapole boson structure functions $\alpha_{\text{dd}}(r)$, $\alpha_{\text{sg}}(r)$, and $\alpha_{\text{dg}}(r)$, extracted for the Nd isotopes from the transition charge densities in Fig.1 and from the IBA calculations described in the text. The last two columns are results with different signs for the transition densities (see text for more details).

A ∂' shape is essentially obtained for all three structure functions. Variations limited to nearly one fm in the central positions and to a factor two in the heights are observed in the surface peaks along the isotopic chain. The shape of the deduced sg structure functions (second row of Fig. 3) is very similar to that of the corresponding experimental transition charge densities in the second row of Fig. 1. This result is consequence of the performed IBA calculations which predict the strongest contribution to the strength of these levels coming from the sg configuration $[Q4\text{SG}(g+\tilde{s} + s+\tilde{g})^{(4)}]$. The deduction of the dd and dg structure functions

is more uncertain, since the levels which have the strongest dd $[(d^+\tilde{d})^{(4)}]$ or dg $[(g^+\tilde{d} + d^+\tilde{g})^{(4)}]$ matrix elements receive the strongest contribution to the strength from the overwhelming sg configuration. Only in A=148 and 150 this does not occur and the deduced $\alpha_{dd}(r)$ is similar in shape to the experimental density of the 4_1^+ state.

A different acceptable solution can be obtained only for $^{142,144,146}\text{Nd}$. In this alternative solution only the structure function $\alpha_{dd}(r)$ results to have a different shape. In the case of ^{142}Nd , $\alpha_{dd}(r)$ has a radial distribution (not reported in Fig. 3) similar to that obtained in the first solution, but with the outer peak three times higher. A shape more complex than a ∂' (last two columns of Fig. 3) is obtained for $^{144,146}\text{Nd}$. In the case of ^{146}Nd the shape is rather similar to that of a ∂'' , but the outer peak is too small. This second solution, more in agreement with the results of Ref. 3 obtained for vibrational nuclei, would suggest a strong variation of the radial behaviour of $\alpha_{dd}(r)$ with the nuclear structure. The observation of a ∂'' shape for $\alpha_{dd}(r)$ in ^{146}Nd is a consequence of an experimental evidence and of the performed IBA calculations. For this nucleus the experimental density, given in the first row of Fig. 1, peaks 0.5 fm outer than the corresponding one in the second row; this is true also for ^{144}Nd and ^{148}Nd , but in ^{146}Nd the dd configuration is more split than in the other isotopes, and, as a consequence, its contribution to the level strength is weak. In this case the experimental transition density can be explained as the sum of a large sg contribution (of ∂' type) and a smaller dd contribution of ∂'' type. In the nuclei where IBA calculations predict a dominant dd contribution, as in ^{148}Nd , $\alpha_{dd}(r)$ necessarily results to have a shape very similar to the experimental charge transition density and therefore of ∂' type.

In summary, hexadecapole transition charge densities with slightly different radial shapes, of ∂' type, have been deduced for all even-even Nd isotopes. The agreement between the experimental and IBA calculated results and the analogies among the shapes of the densities belonging to different isotopes and horizontally displayed in Fig. 1, suggest that at least three of the four L=4 g-boson pair configurations have been identified in the Nd isotopes. The sg configuration, which corresponds to a nuclear hexadecapole vibration, is situated at excitation energies nearly constant with the isotope; also its strength is nearly constant but decreases in the rotational ^{150}Nd . The dd configuration, related to the two-phonon quadrupole excitation, is situated at energies strongly decreasing with the isotope. Parameters with a smooth $N_V \cdot N_\pi$ dependence have been required by the fit procedures for the g-boson strength; this allowed the extraction of g-boson structure functions (first solution, ∂' type) which varied smoothly as a function of isotope. This further emphasises the capability of the *sdg*-IBA model to account for the low-lying hexadecapole strength in regions of different nuclear structures with a limited number of variations.

The author feels indebted with R. De Leo for the clarifying discussions about the subject of the present work and would like to thank N. Blasi, J.A. Bordewijk, M.N. Harakeh, C.W. de Jager, S. Micheletti, M. Pignanelli, R.K.J. Sandor, H. de Vries, S.Y. van der Werf, J. Wesseling, the KVI and NIKHEF-K staffs for the fruitful collaboration.

References

- [1] A. Bohr and B.R. Mottelson, *Nuclear Structure* (W.A. Benjamin, Reading, 1975), Vol. II, and references therein.
- [2] M.A. Moinester *et al.*, Nucl. Phys. **A383**, 264 (1982).
- [3] J. Wesseling *et al.*, Nucl. Phys. **A535**, 285 (1991).
- [4] R.K.J. Sandor *et al.*, Nucl. Phys. **A535**, 669 (1991).
- [5] R. Perrino *et al.*, Nucl. Phys. **A561**, 343 (1993).
- [6] R.K.J. Sandor, Ph.D. Thesis, Vrije Universiteit, Amsterdam (1991), unpublished;
R.K.J. Sandor *et al.*, Phys. Rev. **C43**, R2040 (1991)
- [7] R.K.J. Sandor *et al.*, Nucl. Phys. **A551**, 378 (1993).
- [8] R. Perrino, Tesi di Dottorato, Universita' di Bari, Bari (1992), unpublished;
M. Pignanelli *et al.*, Nucl. Phys. **A559**, 1 (1993).
- [9] O. Scholten, The program-package PHINT, private communication.
- [10] F. Todd Baker *et al.*, Phys. Rev. **C32**, 2212 (1985); Nucl. Phys. **A501**, 546 (1989);
R. De Leo *et al.*, Nucl. Phys. **A504**, 109 (1989); M. Pignanelli *et al.*, Nucl. Phys. **A540**, 27 (1992); P.B. Goldhorn *et al.*, Phys. Lett. **B103**, 291 (1981); A. Sethi *et al.*, Nucl. Phys. **A518**, 536 (1990).
- [11] O. Scholten, Ph.D. Thesis, Rijksuniversiteit, Groningen (1980), unpublished.
- [12] R.F. Casten, W. Frank and P. von Brentano, Nucl. Phys. **A444**, 133 (1985).
- [13] V.G. Soloviev, *Theory of complex nuclei* (Pergamon, Oxford, 1976).
- [14] H. C. Wu *et al.*, Phys. Rev. **C38**, 1638 (1988).